Progress In Electromagnetics Research C, Vol. 33, 243–258, 2012

DESIGN OF OMNIDIRECTIONAL HIGH-GAIN ANTENNA WITH BROADBAND RADIANT LOAD IN C WAVE BAND

S. Lin*, M.-Q. Liu, X. Liu, Y.-C. Lin, Y. Tian, J. Lu, and Z.-H. Zhao

School of Electronics and Information Engineering, Harbin Institute of Technology, Harbin 150080, China

Abstract—Three novel structures of coplanar waveguide (CPW) cross-coupling-fed antenna with different kinds of broadband radiant loads, which are applied in C wave band, are presented. The simulated results by CST MICROWAVE STUDIO® indicate that these structures of antenna are able to expand bandwidth, improve gain and maintain good omnidirectional radiation characteristics while the sizes of the structures are relatively small. The antenna surface current simulated by CST is extracted, explaining the mechanism of broadband, high-gain and omnidirectional radiation characteristics of the antenna. Three structures of antenna with different kinds of broadband radiant loads are designed, manufactured and measured. The antenna is printed on *FR*-4 epoxy substrate with 0.5 mm thickness. According to the measured results of these three structures, the operating bandwidths with a reflection coefficient lower than −10 dB are 4.27∼4.90 GHz, 4.04∼5.07 GHz and 4.05∼4.87 GHz. The relative bandwidths are up to 13.7%, 22.6% and 18.4% respectively. The *H*-plane maximum omnidirectional gains are 6.6 dB (4.8 GHz), 6.8 dB (4.6 GHz) and 7.8 dB (4.6 GHz), and the maximum magnitudes of unroundness are 3.0 dB, 2.8 dB and 2.8 dB (4.5 GHz) respectively. The measured and simulated results do not differ much from each other. The overall sizes of the antennas are 133.5 mm × 14.4 mm (triangular load), 148.2 mm × 18 mm (cutting semi-circular load) and 145.65 mm × 16.1 mm (circular load) respectively, and the gains per electronic length on the polarization direction are 3.1 dB, 3.1 dB and 3.6 dB, which are relatively high. These three structures of antennas are suitable for communication systems working in C wave band.

Received 23 September 2012, Accepted 17 October 2012, Scheduled 18 October 2012

* Corresponding author: Shu Lin (linshu@hit.edu.cn).

1. INTRODUCTION

Omnidirectional antennas are a kind of antennas which can achieve 360° omnidirectional homogeneous radiation in the horizontal plane while the lobes are relatively narrow in the vertical plane. Such antennas are usually used for point-to-multipoint communication. In order to increase the communication distance, the gain of antennas needs to be improved. Meanwhile, the antennas are required to possess a certain beam width in the vertical plane to satisfy the communication coverage. Therefore, the general provision for omnidirectional high-gain antenna is that the omnidirectional gain should be higher than 4 dBi. The researchers have proposed a series of design methods of omnidirectional high-gain antennas: (1) coaxial collinear antenna [1–3]: the antenna adopts multiple coaxial radiators which are coaxially arranged, and the short-circuit component in the terminal provides standing wave current on the coaxial radiators. The gain of antenna improves with the increase in the number of coaxial radiators, which can reach 8 dBi or higher. However, the bandwidth is relatively narrow; (2) printed dipole array antenna fed by balanced microstrip line [4–6]: omnidirectional radiation is achieved by the closely arranged printed dipole array; (3) CPW cross-fed antenna [7]: this is a new kind of antenna which evolved from COCO antenna. By adopting radiant loads, the antenna can obtain a relative bandwidth up to 19.2% and an omnidirectional gain of 5.2 dBi. The antenna works in WLAN frequency band (a part of S wave band), and it is double-sided printed on *FR*-4 epoxy substrate. Also, the design of the antenna introduces the structure of fly line to feed coercively. However, the shortage of the paper is: it did not discuss antennas working in higher frequency band; consequently, whether the *FR*-4 epoxy substrates are suitable for antennas operating in higher frequency cannot be tested. It is generally considered that the *FR*-4 epoxy substrate can only be used in circuit working at frequency lower than 1 GHz, because of the high loss tangent of the *FR*-4 epoxy substrate (magnitude of 10^{-2}). However, if a reasonable structure is adopted, *FR*-4 can be used in occasion of the high operating frequency.

In this paper, a single-sided printed omnidirectional high-gain antenna with broadband radiant load working in C wave band is proposed in order to test the adaptation of *FR*-4 epoxy substrates in high frequency; three types of load structures, triangular, cutting semi-circular and circular load, respectively, are discussed to achieve relatively broad bandwidth; the antenna gain is improved by adopting 6 radiating elements. The index "gain per electronic length" is presented to judge the degree of miniaturization of the antenna. Moreover, the

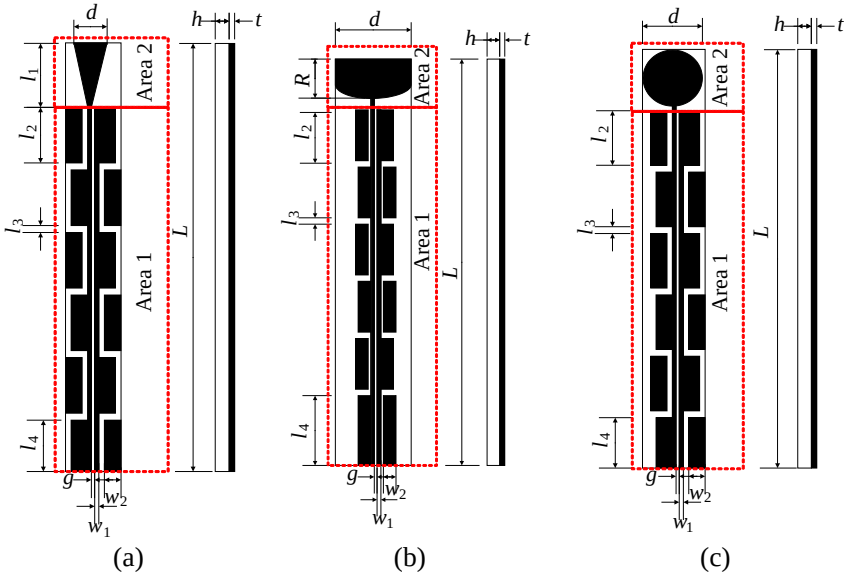

Figure 1. The configuration of the proposed antenna 1∼3, (a) triangular load, (b) cutting semi-circular load, (c) circular load.

paper gives a detailed simulation analysis and test results.

2. ANTENNA STRUCTURE AND WORKING PRINCIPLE

The CPW cross-coupling-fed printed antenna designed in this paper is placed on *FR*-4 epoxy substrate, a material whose dielectric constant $\varepsilon_r = 4.4$, thickness $h = 0.5\,\text{mm}$. The purpose of choosing a substrate as thin as possible is to cut down the dielectric loss. The presented antenna is a single-sided printed circuit board structure. The geometrical configuration and dimensions of the metal patterns (the black area) on the substrate are shown in Figure 1. The entire antenna can be divided into the following two parts: the CPW cross-fed area (area 1) and the terminal radiant load matching area (area 2). The front of the circuit board includes 6 segments of coplanar waveguide feeder elements which are cross-linked together. At the terminal on the top, a radiant metal patch load connects to the central feeder of the coplanar waveguide. The model is built in CST MICROWAVE STUDIO®, and the structural parameters are presented in Tables 1 ∼ 3.

Table 1. Structural parameters of antenna with triangular load (antenna 1).

Parameters	h	t	l_1	l_2	l_3	l_4	g	w_1	w_2	d	L
Dimensions (mm)	0.5	0.1	15	17.25	3	17.25	0.4	0.8	5.8	5	133.5

Table 2. Structural parameters of antenna with cutting semi-circular load (antenna 2).

Parameters	h	t	L	l_2	l_3	l_4	g	w_1	w_2	d	R
Dimensions (mm)	0.5	0.1	148.2	19	2.5	17.25	0.4	0.8	3.1	25	18

Table 3. Structural parameters of antenna with circular load (antenna 3).

Parameters	h	t	L	l_2	l_3	l_4	g	w_1	w_2	d
Dimensions (mm)	0.5	0.1	145.65	18	3.8	18	1.2	1.7	3.3	15.65

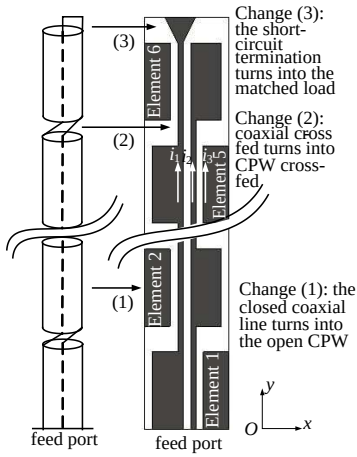

Figure 2. Evolution of the antenna structure.

The proposed antenna shares some similarities with COCO antenna mentioned in literature [2], but the antenna's structure has transformed from three-dimensional to plane printed circuit structure, from enclosed structure to open structure, as shown in Figure 2.

When current is fed to the feeder from the bottom, it flows along the cross-linked transmission lines, establishing a current distribution on the transmission line. When the current flows to the terminal (top), it encounters a radiant metal patch load, establishing a current distribution on the metal patch. Since the radiant metal patch, the CPW metal wire connected thereto and the ground on the left and right together form a monopole antenna, the current above is able to radiate into free space. Therefore, it can be considered that the entire proposed antenna is connected to a matched load on the terminal. Within the operating band of monopole antenna, the current on the CPW cross-linked feeder is traveling wave current, which is the significant difference between the open CPW cross-fed antenna designed in this paper and the traditional COCO antenna. Because of the influence of the terminal short circuit reflection, the current on the traditional COCO antenna is standing wave current. This difference makes the bandwidth of the CPW cross-fed antenna wider than that of the traditional COCO antenna. This traveling wave current establishes a current distribution on the other metal ground of CPW by coupling, and this part of current is standing wave current, whose resonance frequency is limited by the dimension of the ground, l_2 (or l_4, labeled in Figure 1). The resonance frequency can be calculated by Formula (1). ε_e in the formula stands for effective dielectric constant considering the influence of the medium.

$$f = \frac{c}{2l_i\sqrt{\varepsilon_e}}, \quad i = 2, 4 \tag{1}$$

As shown in Figure 2, for one element of the antenna, three parts of current flowing in $+y$ direction can be obtained by the simulation of CST MWS®, including i_1, i_2 and i_3. The amplitude of these three parts of current is relatively large, which plays a decisive role in the radiation of the antenna. Wherein the current of i_1 and i_2 are equal in amplitude and opposite in phase, thus these two parts of current radiation get counteract, and the radiation of coupling current i_3 determines radiation pattern and other characteristics of the antenna. According to the discussion above, in order to increase the antenna gain, it is necessary to control the phase of i_3 in each element by adjusting the space between feeding positions l_3, which makes them in-phase stack in the far field. Moreover, the length of antenna elements l_2 determines the resonant frequency of i_3, so the working frequency of the antenna can be adjusted by changing the length of antenna elements.

One thing to note here is that the analysis is the same as in [7], but the distinction between the antenna in this paper and [7] is that the proposed antenna is free of metal fly line. This ensures the

electromagnetic wave's propagation in the medium as little as possible, which decreases the dielectric loss and improves the efficiency of the antenna.

3. SIMULATION AND ANALYSIS

3.1. Simulated Results of Radiant Load

Figure 3 shows the simulated results of electromagnetic properties of radiant metal patch load fed by CPW. The simulated results show that the $|S_{11}|$ of load is less than -6 dB in the frequency range of 4∼5 GHz, which indicates that the load is equivalent to a kind of broadband matched load. Antennas with this kind of load should belong to the scope of traveling wave antennas. However, different from traditional traveling wave antenna, this kind of antenna load belongs to radiant load, and the simulated results shown in Figure 4

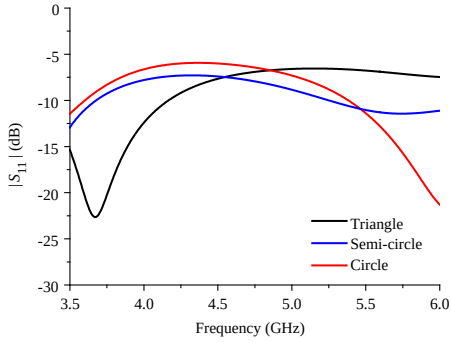

Figure 3. The simulated $|S_{11}|$ with three radiant loads.

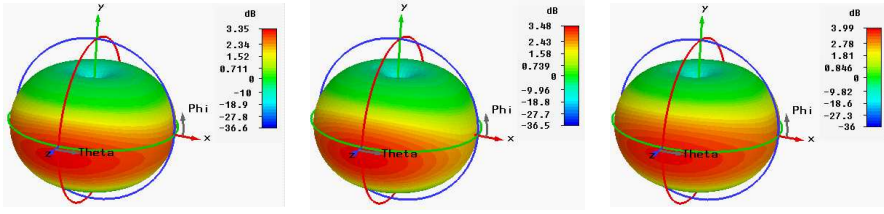

Figure 4. The simulated radiation characteristics of antenna 1∼3 (at 4.5 GHz), vertical axis unit: dB. (a) Antenna 1. (b) Antenna 2. (c) Antenna 3.

prove this conclusion. Because the currents on the load and the feed line flow in the same direction, their radiation fields share the same polarization mode. That's why the antenna proposed in this paper achieves relatively high radiation efficiency.

3.2. Simulated Results of Antenna with Radiant Load

Since all three kinds of proposed radiant loads have relatively broad bandwidth, and have relatively small size on the polarization direction, all of them can be used for the load of CPW cross-fed antenna. Next, three of the loads will be introduced into the design of antennas respectively.

Figure 5 shows the simulated reflection coefficient of these three kinds of antennas. The operating bandwidths of antenna 1∼3 with a reflection coefficient less than −10 dB are 4.23∼4.86 GHz, 4.00∼5.16 GHz and 3.99∼4.96 GHz while the relative bandwidths are

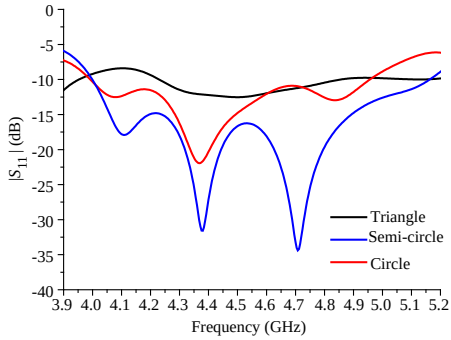

Figure 5. The simulated $|S_{11}|$ of the proposed antennas.

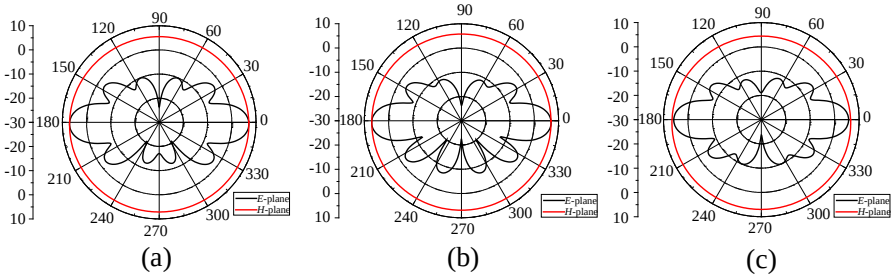

Figure 6. The simulated results of gain pattern (at 4.5 GHz), vertical axis unit: dB. (a) Antenna 1. (b) Antenna 2. (c) Antenna 3.

Table 4. Summary on radiation characteristics of antenna 1∼3.

Type of Antenna	Frequency Band with Omnidirectional Gain Higher Than 4.0 dB	Gain Pattern Bandwidth	Maximum Gain within the Frequency Band
Antenna 1	4.5∼5.0 GHz	10.5%	7.4 dB (at 4.7 GHz)
Antenna 2	4.3∼4.7 GHz	8.9%	7.8 dB (at 4.7 GHz)
Antenna 3	4.4∼4.8 GHz	8.7%	8.7 dB (at 4.8 GHz)

up to 13.9%, 25.3% and 21.7% respectively. The results show that the impedance bandwidths of these three kinds of antennas with loads do not differ greatly, which bring more flexibility to the design of antennas that we can focus on other aspects of performance.

Figure 6 shows the simulated radiation pattern of the three kinds of antennas on E-plane and H-plane at typical frequency point 4.5 GHz. It can be obtained that the antennas have achieved omnidirectional radiation on H-plane and lower side lobes on E-plane.

Table 4 makes a summary on the radiation characteristics of antenna 1∼3, it can be seen that: although the impedance bandwidths of the antennas are relatively broad, the gain pattern bandwidths decrease significantly, and the difference among the gain pattern bandwidths of the three antennas is not much. The reason for this phenomenon is mainly related to the current distribution on the radiant elements of the antennas, which will be explained in Section 3.3. Gain and pattern here are two parameters closely connected, and the omnidirectional gain refers to the gain where the antenna radiation is the weakest on H-plane. The decrease of omnidirectional gain means that the un-roundness of the antenna pattern increases and that omnidirectionality gets worse.

3.3. The Simulated Results and Analysis of the Antenna Metal Surface Current

According to the analysis of antenna's working principle in Section 3.2, the antenna impedance characteristics and radiation characteristics can be explained by the simulation of the antenna surface current by CST. Figure 7 presents the simulated results of the metal surface current of antenna 1∼3 (at 4.5 GHz) and the current phase distribution curve on transmission line which is part of the coplanar waveguide cross-fed area. At typical frequency 4.5 GHz, the simulated results

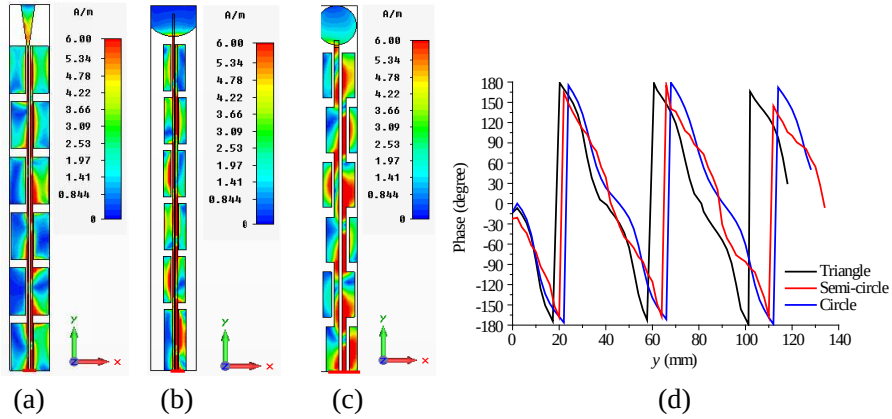

Figure 7. The simulated results of metal surface current for antenna 1∼3, (a) antenna 1 (at 4.5 GHz), (b) antenna 2 (at 4.5 GHz), (c) antenna 3 (at 4.5 GHz), (d) current phase on the transmission line of the coplanar waveguide cross-fed area.

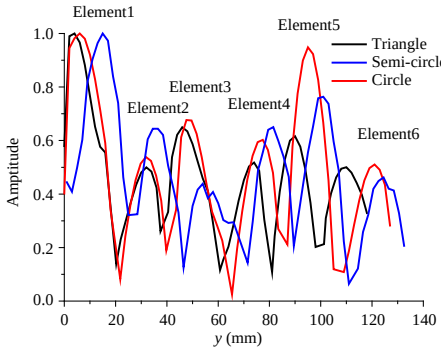

Figure 8. Normalized current amplitude distribution on the 6 radiant elements of the proposed antennas (at 4.5 GHz).

of phase change a lot, which indicate that the current is traveling wave current, due to the broadband matched load mentioned above connecting to the terminal. This traveling wave current couples to the isolate ground which is not cross-fed by the coplanar waveguide, and thus forming standing wave current (Figure 8, at 4.5 GHz) as well as deciding the antenna radiation characteristics. Table 5 shows the current amplitude and phase of the 6 radiant elements' isolate ground edge respectively for antenna 1∼3. It can be seen that the current amplitude of the 6 elements do not differ much from each

Table 5. Normalized current amplitude and phase on the 6 radiant elements at 4.5 GHz.

Element Number		1	2	3	4	5	6
Antenna 1	Normalized Current Amplitude	1.00	0.50	0.65	0.52	0.62	0.50
	Phase (rad)	2.57	2.32	2.29	2.69	1.98	1.59
Antenna 2	Normalized Current Amplitude	1.00	0.64	0.44	0.65	0.76	0.46
	Phase (rad)	1.37	0.81	0.98	0.60	1.29	1.06
Antenna 3	Normalized Current Amplitude	1.00	0.53	0.68	0.6	0.95	0.51
	Phase (rad)	0.5	1.09	0.32	0.42	0.38	1.23

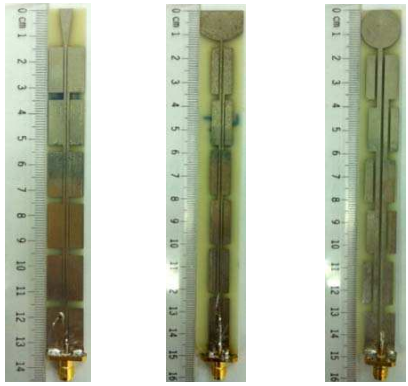

Figure 9. The prototypes of antenna 1∼3, (a) antenna 1, (b) antenna 2, (c) antenna 3.

other at 4.5 GHz, and they are almost in-phase or the phase difference among them is lower than $\pi/2$. This shows that here the antennas are equivalent to the broadside array antennas composed of dipole antennas in radiation way, which can form omnidirectional radiation.

The current on the transmission line of the coplanar waveguide cross-fed area establishes induced current on the sideward isolate metal radiant elements 1∼6. This current produces radiation and finally forms the radiation pattern of the antenna. Though the induced current is standing wave current, its phase is still affected by the traveling wave current flowing on the transmission line. As the offset of frequency increases, it will lead to the excessive deviation of current phase among the elements (greater than 90°), which breaks

the requirement for broadside array antenna and makes the radiation pattern of the antenna unsatisfiable.

4. MEASURED RESULTS

Three of the manufactured antennas (Figure 9) were measured by Agilent E8363B Vector Network Analyzer in microwave anechoic chamber, and the results are shown in Figure 10 and Figure 11. Figure 10 presents the measured results of antenna reflection coefficient, which shows that the operating bands ($|S_{11}| < -10\,\text{dB}$) are 4.27∼4.90 GHz, 4.04∼5.07 GHz and 4.05∼4.87 GHz respectively and the relative bandwidths are 13.7%, 22.6% and 18.4% respectively. The results show that: (1) the measured results of the operating bandwidth do not differ much from the simulated ones, but there is a certain discrepancy between the resonance depths obtained by the measurement and simulation, and this is due to the loss

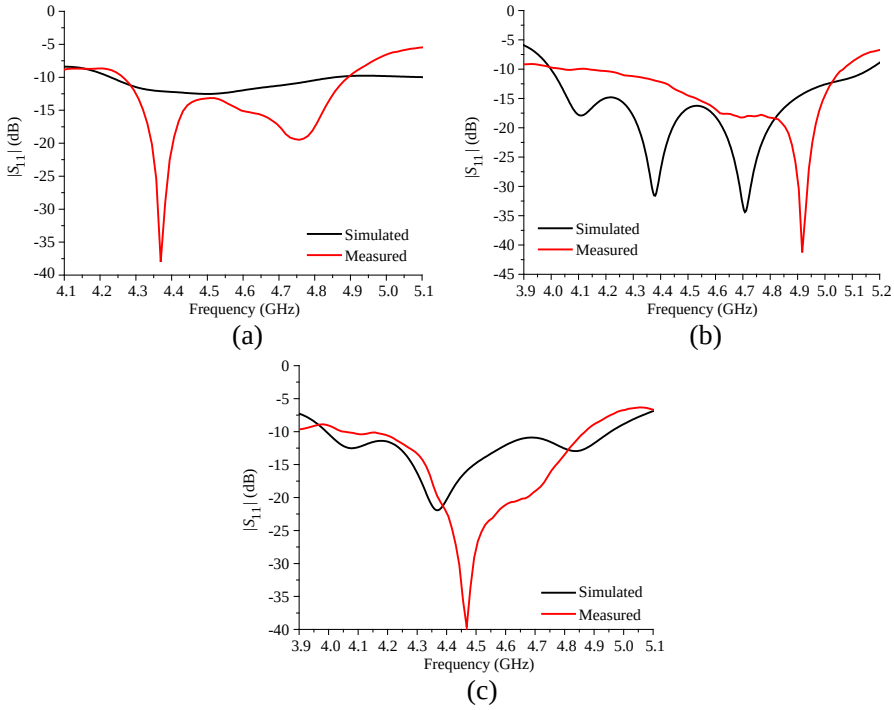

Figure 10. The measured results of reflection coefficient for antenna 1∼3, (a) antenna 1, (b) antenna 2, (c) antenna 3.

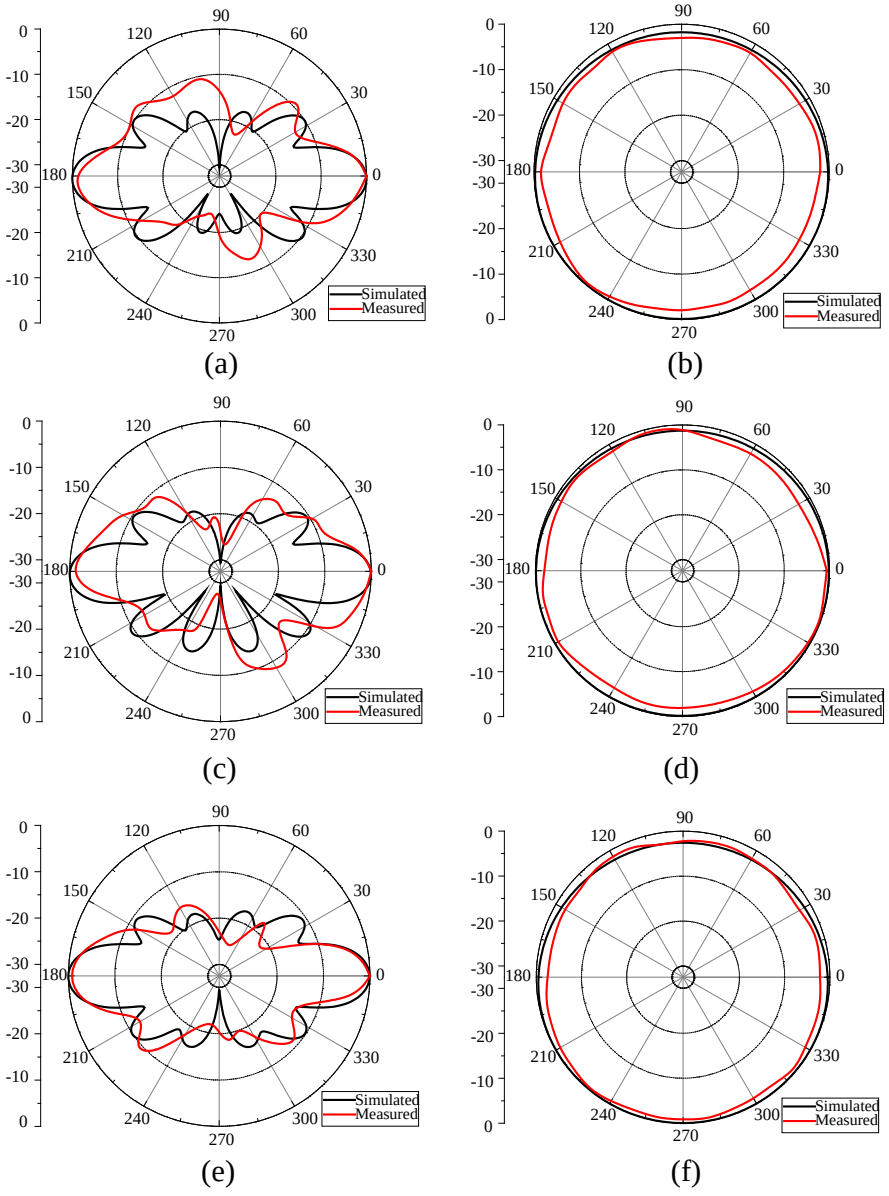

Figure 11. The measured radiation patterns of antenna 1∼3, vertical axis unit: dB. (a) 4.5 GHz, *E*-plane, antenna 1. (b) 4.5 GHz, *H*-plane, antenna 1. (c) 4.5 GHz, *E*-plane, antenna 2. (d) 4.5 GHz, *H*-plane, antenna 2. (e) 4.5 GHz, *E*-plane, antenna 3. (f) 4.5 GHz, *H*-plane, antenna 3.

Table 6. The measured results of gains for antenna 1∼3.

Frequency(GHz)		4.4	4.5	4.6	4.7	4.8
Antenna 1	Simulated value (dB)	6.3	6.9	7.3	7.4	7.0
	Measured value (dB)	6.0	6.5	6.5	6.2	6.6
Antenna 2	Simulated value (dB)	6.2	7.0	7.5	7.8	7.5
	Measured value (dB)	6.0	6.5	6.8	5.9	4.9
Antenna 3	Simulated value (dB)	7.0	7.8	8.3	8.5	8.7
	Measured value (dB)	6.3	7.4	7.8	7.1	6.8

and inhomogeneity of the *FR*-4 epoxy substrate; (2) despite of the discrepancy of the resonance depth, both the measured and simulated $|S_{11}|$ are lower than -10 dB, which is to say the antenna reflected power is lower than 10%. So that the discrepancy is lower than 10%, which means that in the design method of this paper, the instability of FR-4 epoxy substrates does not affect antenna impedance characteristics much.

Figure 11 gives the measured results of antenna normalized radiation pattern on *E*-plane and *H*-plane. In the measured results, the un-roundness on *H*-plane is generally bigger, and this is caused by two aspects of reasons: (1) the materials selected in the antenna simulation are all ideal conductor and ideal medium, but the substrate material adopted in practice is lossy medium; (2) the relative permittivity of the antenna substrate is asymmetric. These indicate that the instability of *FR*-4 epoxy substrates affects the measured results of antenna radiation pattern. The measured gains of antenna 1∼3 are presented in Table 6. Compared to the simulated results, the gains have declined, but the declination is not in large scale, showing that lossy medium will cause the declination of antenna gain. However, the thickness of the substrates picked in this paper is relatively small, so that the loss is little and the declination of gain is not much.

The measured results of reflection coefficient, radiation pattern and gain show that the *FR*-4 epoxy substrate is suitable for the proposed antenna to work in relatively high frequency.

5. SPECIALTY OF THE PROPOSED ANTENNA

In order to compare the indexes of different types of antennas, this paper proposed the parameter "gain per electronic length" apart from using the relative value — relative bandwidth. This new parameter

can be defined by formula (2):

$$K = \frac{\lambda}{L}G \tag{2}$$

In the formula,

K — gain per electronic length.
L — height of antenna.
λ — operating wavelength.
G — gain when the operating wavelength is λ.

Since most of the omnidirectional antennas have higher gain when the heights are higher, the parameter K can be used to compare omnidirectional antennas operating in different wave band. The greater the value of K is, the higher the gain per electronic length an antenna can get. Therefore, when the antenna gain satisfies the requirement, antenna with greater value of K has a relatively small height, in other words, has the characteristic of miniaturization.

Table 7 presents the results of comparison between the omnidirectional antennas in this paper and other literatures. It can be seen that the introduction of broadband radiant load improves the efficiency of the proposed antenna in this paper which makes it better than other antennas in aspects of bandwidth and extent of miniaturization.

Table 7. Comparison between omnidirectional high-gain antennas in this paper and other literatures.

Antenna Type	Operating Bandwidth	Relative Bandwidth (%)	Gain at Typical Frequency	Antenna Size (Electrical length)	Omnidirectional Gain per Wavelength at Typical Frequency
Antenna 1	4.27~4.90 GHz	13.7	6.7 dBi (4.8 GHz)	133.5 mm×14.4 mm×0.5 mm (2.14λ ×14.4 mm×0.5 mm)	3.1 dBi/λ (4.5 GHz)
Antenna 2	4.04~5.07 GHz	22.6	6.8 dBi (4.5 GHz)	148.2 mm×18 mm×0.5 mm (2.22λ ×18 mm×0.5 mm)	3.1 dBi/λ (4.6 GHz)
Antenna 3	4.05~4.87 GHz	18.4	8.0 dBi (4.6 GHz)	145.65 mm×16.1 mm×0.5 mm (2.23λ ×16.1mm×0.5mm)	3.6 dBi/λ (4.6 GHz)
The Antenna in [8]	2.38~2.70 GHz	15.1	6.51 dBi (2.4 GHz)	304 mm×20 mm×0.8 mm (2.43λ ×20mm×0.8mm)	2.7 dBi/λ (2.4 GHz)
The Antenna in [9]	2.010~2.025 GHz	0.74	9.9 dBi (2.020 GHz)	860 mm×16 mm×1.5 mm (5.79λ ×16mm×1.5mm)	1.7 dBi/λ (2.020 GHz)
The Antenna in [10]	5.68~5.95 GHz	4.6	10 dBi (5.8 GHz)	300 mm×15.2 mm×2 mm (5.80λ ×15.2mm×2mm)	1.7 dBi/λ (5.8 GHz)

6. CONCLUSION

Three kinds of broadband omnidirectional high-gain antennas with broadband radiant loads are presented. The antennas are manufactured with *FR*-4 epoxy printed substrates. The broadband loads improve the antenna impedance bandwidths up to 20% without decreasing the antenna efficiency. By the influence of the phase of the feeding current, the radiation pattern bandwidths of antennas are less than the impedance bandwidths, which are approximately 10%. Moreover, the parameter gain per electronic length can measure the miniaturization extent of omnidirectional antennas in different types. The greater the parameter is, the higher the miniaturization extent an antenna can obtain. The instability of *FR*-4 epoxy substrates has little effect on antenna in the design method of this paper, which realized the application of *FR*-4 epoxy substrates in the design of antennas operating in C wave band. The proposed antennas in this paper can be widely applied in point-to-multipoint communication by virtue of characteristics including broad bandwidth, high gain and miniaturization.

ACKNOWLEDGMENT

The authors would like to express their sincere gratitude to CST Ltd., Germany, for providing the CST Training Center (Northeast China Region) at our university with a free package of CST MWS® software.

The authors would also like to express their sincere gratitude to "the Fundamental Research Funds for the Central Universities" (Grant No. HIT.NSRIF.2010096).

REFERENCES

1. Yu, C., W. Hong, Z. Kuai, and H. Wang, "Ku-band linearly polarized omnidirectional planar filtenna," *IEEE Antennas and Wireless Propagation Letters*, Vol. 11, 310–313, 2012.
2. Zhou, Y., P. Lee, F. Jia, and B. Xu, "A technique for improving bandwidth of COCO antenna array," *IEEE 4th International Conference on Wireless Communications, Networking and Mobile Computing*, 1–2, Oct. 12–14, 2008.
3. Mishoostin, B. A., V. G. Slyozkin, and E. A. Redkina, "The coaxial collinear antenna with series slot feeding scheme," *IEEE 14th International Crimean Conference on Microwave and Telecommunication Technology*, 352–353, Russia, Sep. 13–17, 2004.

4. Tan, D., W. Hong, J. Chen, L. Tian, P. Yan, J. Zhou, and Z. Kuai, "Wideband omnidirectional printed dipole array antenna," *IEEE 8th International Symposium on Antennas, Propagation and EM Theory (ISAPE)*, 111–113, Nov. 2–5, 2008.
5. Wei, K., Z. Zhang, W. Chen, Z. Feng, and M. F. Iskander,, "A triband shunt-fed omnidirectional planar dipole array," *IEEE Antennas and Wireless Propagation Letters*, Vol. 9, 850–853, 2010.
6. Yu, X., D. Ni, Y. Wu, and F. Z hang, "A novel omnidirectional high-gain printed antenna," *Radar Science and Technology*, Vol. 4, No. 4, 232–235, China, Aug. 2006.
7. Lin, S., G.-L. Huang, R.-N. Cai, X.-Y. Zhang, and X.-Q. Zhang, "Design of novel CPW cross-fed antenna," *Progress In Electromagnetics Research C*, Vol. 23, 191–203, 2011.
8. Wang, L., K. Wei, J. Feng, Z. Zhang, and Z. Feng, "A wideband omnidirectional planar microstrip antenna for WLAN applications," *IEEE Conference on Electrical Design of Advanced Packaging and Systems Symposium (EDAPS)*, 1–4, Dec. 12–14, 2011.
9. Yu, X., D. Ni, and W. Wang, "An omnidirectional high-gain antenna element for TD-SCDMA base station," *ISAPE'06, 7th International Symposium on Antennas, Propagation & EM Theory*, 1–4, Oct. 26–29, 2006.
10. Chen, X., K. Huang, and X.-B. Xu, "A novel planar slot array antenna with omnidirectional pattern," *IEEE Transactions on Antennas and Propagation*, Vol. 59, No. 12, 4853–4857, Dec. 2011.